TABLE 11.3 (Continued)

Gene	Description	FC	*p*	PKA	PKC
DOWNREGULATION					
Hmgb2	High mobility group box 2	0.45	0.0008	+	−
Ptn	Pleiotrophin	0.45	0.0008	+	−
Aldh1a1	Aldehyde dehydrogenase family 1, subfamily A1	0.46	0.0008	+	+
Pbx3	Pre B-cell leukemia transcription factor 3	0.47	0.0008	+	+
Slc12a2	Solute carrier family 12, member 2	0.50	0.0008	−	−

Abbreviations: FC, fold change; PKA, protein kinase A; PKC, protein kinase C.
Modified data published by Schimmer BP, Cordova M, Cheng H, et al. Endocrinology *2006; **147**: 2357–67.*

fasciculata of 9-week-old male rats, using laser capture microdissection (LCM) and a rat cDNA microarray with 22,523 probes.[23] They found 235 and 231 transcripts upregulated more than two-fold in the zona glomerulosa and zona fasciculata, respectively, with an FDR less than 0.05 (Table 11.4). *Frzb*, which inhibits Wnt signaling, was differentially expressed in the zona fasciculata. In contrast, *Wnt4* showed a trend of upregulation in zona glomerulosa cells. Lack of functional WNT4/Wnt4 results in adrenal dysgenesis and compromised aldosterone synthesis in human patients with the female sex reversal and dysgenesis of kidneys, adrenals, and lungs (SERKAL) syndrome and knockout mice lacking Wnt4, respectively.[24,25] It has been inferred that Frzb and Wnt4 inversely modulate adrenal zonation during organogenesis and aldosterone synthesis after birth. Information on zone-specific changes in transcripts will help clarify the development and maintenance of adrenal zonation.

TRANSCRIPTOME ANALYSIS OF ADRENOCORTICAL CELLS IN A MOUSE MODEL OF HUMAN LIPOID ADRENAL HYPERPLASIA

Undoubtedly, mouse models of human disorders would help identify the pathophysiology of disorders and even help determine possible approaches for potential new treatments. Human adrenal glands are not easily accessible and are rarely removed except in cancer, thus making a knockout animal with adrenal insufficiency particularly valuable. One such model, knockout mice lacking steroidogenic acute regulatory protein (StAR), has been described here in detail.

Congenital lipoid adrenal hyperplasia (lipoid CAH) is an autosomal recessive disease due to *STAR* gene mutations. StAR regulates the rate-limiting step of steroidogenesis to facilitate the translocation of newly synthesized cholesterol from the outer to inner mitochondrial membrane.[17,26–28] Patients with lipoid CAH and knockout mice lacking StAR (*Star*$^{-/-}$ mice) exhibit significant defects in steroid hormone biosynthesis and diffuse accumulation of cholesterol esters in the cytoplasm of adrenocortical or gonadal steroidogenic cells.[29–33] Bose *et al.*[29] proposed the "two-hit" model, in which the first hit is loss of StAR-dependent steroidogenesis due to StAR deficiency and the second hit is loss of StAR-independent steroidogenesis caused by accumulated cholesterol esters, thus explaining the varying phenotypes among steroidogenic tissues. However, the molecular mechanisms underlying the cholesterol translocation by StAR and the abrogation of StAR-independent steroidogenesis by cholesterol deposits require clarification. Thus, the transcriptome of steroidogenic cells in the adrenal glands of *Star*$^{-/-}$ mice

TABLE 11.4 Genes Significantly Upregulated in Rat Zona Glomerulosa or Zona Fasciculata by cDNA Microarray

Gene	Description	FC	*p*
ZONA GLOMERULOSA			
Cyp11b2	*Rattus norvegicus* cytochrome P450, family 11, subfamily B, polypeptide 2 (Cyp11b2), nuclear gene encoding mitochondrial protein, mRNA	214.2	0.00078
Rgs4	*Rattus norvegicus* regulator of G-protein signaling 4 (Rgs4), mRNA	68.4	0.00052
Smoc2_predicted	PREDICTED: *Rattus norvegicus* SPARC related modular calcium binding 2 (predicted), transcript variant 2 (Smoc2_predicted), mRNA	49.3	0.00777
Mia1	PREDICTED: *Rattus norvegicus* melanoma inhibitory activity 1 (Mia1), mRNA	43.1	0.00031
Dlk1	*Rattus norvegicus* delta-like 1 homolog (*Drosophila*) (Dlk1), mRNA	38.3	0.00531
Sstr2	*Rattus norvegicus* somatostatin receptor 2 (Sstr2), mRNA	37.2	0.00852
Cadps	*Rattus norvegicus* Ca2+-dependent secretion activator (Cadps), mRNA	33.7	0.00483
LOC311772	PREDICTED: *Rattus norvegicus* similar to nidogen 2 (LOC311772), mRNA	33.6	0.00083
Igsf1	*Rattus norvegicus* immunoglobulin superfamily, member 1 (Igsf1), mRNA	32.9	0.00078
LOC362564	PREDICTED: *Rattus norvegicus* hypothetical LOC362564 (LOC362564), mRNA	31.1	0.00296
Gpc3	*Rattus norvegicus* glypican 3 (Gpc3), mRNA	30.6	0.01434
Cpxm2_predicted	PREDICTED: *Rattus norvegicus* carboxypeptidase X 2 (M14 family) (predicted) (Cpxm2_predicted), mRNA	29.1	0.01163
Atp10a	PREDICTED: *Rattus norvegicus* ATPase, class V, type 10A, transcript variant 1 (Atp10a), mRNA	28.8	0.00118
Postn_predicted	PREDICTED: *Rattus norvegicus* periostin, osteoblast specific factor (predicted) (Postn_predicted), mRNA	24.1	0.02619
Boc_predicted	PREDICTED: *Rattus norvegicus* biregional cell adhesion molecule-related/ downregulated by oncogenes (Cdon) binding protein (predicted) (Boc_predicted), mRNA	23.3	0.00604
RGD1566317_predicted	PREDICTED: *Rattus norvegicus* similar to Tescalcin (predicted) (RGD1566317_predicted), mRNA	22.9	0.00149
Ndn	*Rattus norvegicus* necdin (Ndn), mRNA	19.9	0.00318
Dpt_predicted	PREDICTED: *Rattus norvegicus* dermatopontin (predicted) (Dpt_predicted), mRNA	18.5	0.01768
Kcnn2	*Rattus norvegicus* potassium intermediate/small conductance calcium-activated channel, subfamily N, member 2 (Kcnn2), mRNA	17.5	0.00582
Rbp1	*Rattus norvegicus* retinol binding protein 1, cellular (Rbp1), mRNA	17.4	0.00375
Wfdc1	*Rattus norvegicus* WAP four-disulfide core domain 1 (Wfdc1), mRNA	15.7	0.01163
Acy3	*Rattus norvegicus* aspartoacylase (aminoacylase) 3 (Acy3), mRNA	15.6	0.01682
RGD1307506_predicted	PREDICTED: *Rattus norvegicus* similar to RIKEN cDNA 2310016C16 (predicted) (RGD1307506_predicted), mRNA	15.1	0.00299
Ptgis	*Rattus norvegicus* prostaglandin I2 (prostacyclin) synthase (Ptgis), mRNA	14.9	0.01147

(*Continued*)

TABLE 11.4 (Continued)

Gene	Description	FC	*p*
Reck_predicted	PREDICTED: *Rattus norvegicus* reversion-inducing-cysteine-rich protein with kazal motifs (predicted) (Reck_predicted), mRNA	14.5	0.01353
RGD1564008_predicted	PREDICTED: *Rattus norvegicus* similar to dapper 1 (predicted) (RGD1564008_predicted), mRNA	13.2	0.00483
Nr0b1	*Rattus norvegicus* nuclear receptor subfamily 0, group B, member 1 (Nr0b1), mRNA	12.7	0.01434
Fmod	*Rattus norvegicus* fibromodulin (Fmod), mRNA	12.6	0.02731
Pde2a	*Rattus norvegicus* phosphodiesterase 2A, cGMP-stimulated (Pde2a), mRNA	12.6	0.00184
Dab2	*Rattus norvegicus* disabled homolog 2, mitogen-responsive phosphoprotein (Drosophila) (Dab2), mRNA	12.4	0.00420
ZONA FASCICULATA			
LOC363306	PREDICTED: *Rattus norvegicus* similar to RIKEN cDNA 4930555G01 (LOC363306), mRNA	19.30	0.01525
Ddah1	*Rattus norvegicus* dimethylarginine dimethylaminohydrolase 1 (Ddah1), mRNA	16.21	0.00369
LOC498373	PREDICTED: *Rattus norvegicus* similar to RIKEN cDNA 1700001E04 (LOC498373), mRNA	15.55	0.01342
Cidea_predicted	PREDICTED: *Rattus norvegicus* cell death-inducing DNA fragmentation factor, alpha subunit-like effector A (predicted) (Cidea_predicted), mRNA	15.54	0.00176
Hpx	*Rattus norvegicus* hemopexin (Hpx), mRNA	15.43	0.01921
Hamp	*Rattus norvegicus* hepcidin antimicrobial peptide (Hamp), mRNA	15.32	0.03461
RGD1562717_predicted	PREDICTED: *Rattus norvegicus* similar to ABI gene family, member 3 (NESH) binding protein (predicted) (RGD1562717_predicted), mRNA	14.90	0.00572
Cyp4f4	*Rattus norvegicus* cytochrome P450, family 4, subfamily f, polypeptide 4 (Cyp4f4), mRNA	14.60	0.03031
Serpina11	*Rattus norvegicus* serine (or cysteine) peptidase inhibitor, clade A (alpha-1 antiproteinase, antitrypsin), member 11 (Serpina11), mRNA	13.03	0.00670
LOC501497	PREDICTED: *Rattus norvegicus* LOC501497 (LOC501497), mRNA	11.73	0.00630
Fabp6	*Rattus norvegicus* fatty acid binding protein 6, ileal (gastrotropin) (Fabp6), mRNA	11.35	0.02633
Nkx6-2_predicted	PREDICTED: *Rattus norvegicus* NK6 transcription factor related, locus 2 (Drosophila) (predicted) (Nkx6-2_predicted), mRNA	10.04	0.00385
RGD1560609_predicted	PREDICTED: *Rattus norvegicus* similar to Vanin-3 (predicted) (RGD1560609_predicted), mRNA	9.79	0.03668
Frzb	PREDICTED: *Rattus norvegicus* frizzled-related protein (Frzb), mRNA	9.45	0.00565
LOC363060	*Rattus norvegicus* similar to RIKEN cDNA 1600029D21 (LOC363060), mRNA	9.31	0.03191
Ephb6	PREDICTED: *Rattus norvegicus* Eph receptor B6 (Ephb6), mRNA	9.07	0.00770
Fbxo17	*Rattus norvegicus* F-box only protein 17 (Fbxo17), mRNA	9.03	0.00483

(*Continued*)

TABLE 11.4 (Continued)

Gene	Description	FC	*p*
Rab33a_predicted	PREDICTED: *Rattus norvegicus* RAB33A, member of RAS oncogene family (predicted) (Rab33a_predicted), mRNA	8.99	0.01338
Hhex	*Rattus norvegicus* hematopoietically expressed homeobox (Hhex), mRNA	8.96	0.02417
Vnn1	*Rattus norvegicus* vanin 1 (Vnn1), mRNA	8.80	0.00777
Hsd11b2	*Rattus norvegicus* hydroxysteroid 11-beta dehydrogenase 2 (Hsd11b2), mRNA	8.26	0.00589
Mt1a	*Rattus norvegicus* metallothionein 1a (Mt1a), mRNA	8.17	0.00876
Macrod1	*Rattus norvegicus* MACRO domain containing 1 (Macrod1), mRNA	7.99	0.00247
Edg4_predicted	PREDICTED: *Rattus norvegicus* endothelial differentiation, lysophosphatidic acid G protein-coupled receptor 4 (predicted) (Edg4_predicted), mRNA	7.88	0.00483
Dhcr7	*Rattus norvegicus* 7-dehydrocholesterol reductase (Dhcr7), mRNA	7.15	0.00486
LOC681153	PREDICTED: *Rattus norvegicus* hypothetical protein LOC681153 (LOC681153), mRNA	6.96	0.03839
Arih1	*Rattus norvegicus* ariadne ubiquitin-conjugating enzyme E2 binding protein homolog 1 (*Drosophila*) (Arih1), mRNA	6.85	0.01501
F11r	*Rattus norvegicus* F11 receptor (F11r), mRNA	6.76	0.01682
Comtd1_predicted	PREDICTED: *Rattus norvegicus* catechol-O-methyltransferase domain containing 1 (predicted) (Comtd1_predicted), mRNA	6.70	0.02182
Amid_predicted	PREDICTED: *Rattus norvegicus* apoptosis-inducing factor (AIF)-like mitochondrion-associated inducer of death (predicted) (Amid_predicted), mRNA	6.49	0.04764

Abbreviation: FC, fold change.
Modified data published by Nishimoto K, Rigsby CS, Wang T, et al. Endocrinology *2012; 153: 1755–63.*

could help identify related biological pathways that may help elucidate the pathophysiology of StAR deficiency. The following subsection is a review of findings published previously.[34]

Targeted Expression of eGFP in Adrenocortical Cells

In order to collect pure adrenocortical cells, Ishii *et al.* generated transgenic mice carrying a bacterial artificial chromosome (BAC) transgene targeting eGFP to steroidogenic cells under the control of endogenous regulatory sequences from the mouse *Star* gene (StAR/eGFP mice).[34] For transgene construction, eGFP cDNA was inserted into the coding region of *Star* in a BAC clone containing the mouse *Star* gene with 47 kb of the 5′-flanking region and 62 kb of the 3′-flanking regions (StAR/eGFP BAC) (Figure 11.2A). Anti-eGFP antibody immunoreactivity and intrinsic eGFP fluorescence were observed in the adrenocortical cells, the interstitial cells of testes, and the theca cells, luteal cells, and stromal cells of ovaries from mice carrying the StAR/eGFP BAC transgene (Figure 11.2B), consistent with the endogenous StAR expression. The adrenal glands were dissected from wild type ($Star^{+/+}$) embryos or $Star^{-/-}$ embryos with the StAR/eGFP BAC transgene at embryonic day (E) 17.5 or E18.5. Single cell

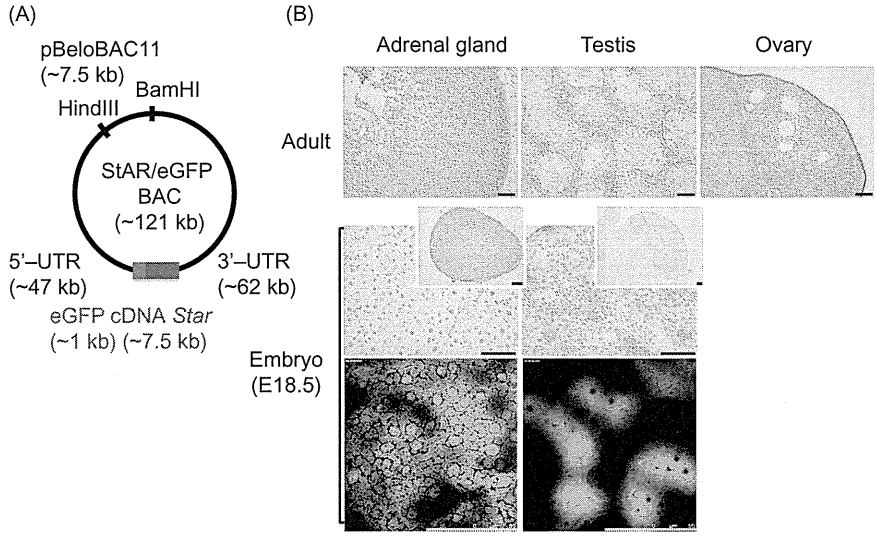

FIGURE 11.2 (A) Structure of the StAR/eGFP bacterial artificial chromosome (BAC) transgene. (B) Expression of the StAR/eGFP BAC transgene in adrenal glands and gonads from adults (top) or embryos at E18.5 (middle and bottom). Pictures in the top and middle show immunohistochemical staining for GFP expression in bright field lighting; those in the bottom demonstrate GFP fluorescence in dark field lighting. Each smaller picture in the middle shows a lower magnification view of the larger picture. Scale bars are 100 μm.

suspensions were prepared by enzymatic dissociation. eGFP-positive cells were selectively isolated by fluorescence-activated cell (FAC) sorting. Cell suspensions from the adrenal glands of $Star^{+/+}$ or $Star^{-/-}$ mice carrying no StAR/eGFP transgene were used as negative controls in FAC sorting to exclude the possibility of macrophage contamination due to autofluorescence.[35] StAR/eGFP mice provide a useful strategy for selective purification of StAR-expressing steroidogenic cells from the adrenal glands.

Differentially Regulated Genes in Mouse cDNA Microarrays

Ishii *et al.* determined the transcriptome of the adrenocortical cells of $Star^{+/+}$ or $Star^{-/-}$ mice using a Whole Mouse Genome Microarray G4122F, Cy3-labeled cRNAs (One-Color Quick Amp Labeling kit), and a Gene Array Scanner (all from Agilent Technologies, Inc., Palo Alto, CA).[34] The data were analyzed using the Gene Spring GX 11.5.1 software (Agilent Technologies, Inc.). The difference in gene expression was assessed by averaging the normalized values and performing a pairwise analysis between $Star^{+/+}$ mice and $Star^{-/-}$ mice. DEGs were defined as having a gene expression ratio of $\geq$2-fold and a p value evaluated by FDR $<$0.2.[12] The transcriptome analysis identified 1973 DEGs (1206 upregulated and 767 downregulated) between $Star^{+/+}$ and $Star^{-/-}$ mice (Figure 11.1).

The expression levels of the selected genes were validated by quantitative polymerase chain reaction (qPCR) using additional samples of FAC-sorted cells from the adrenal glands at E17.5 or E18.5. The relative gene expression in $Star^{+/+}$ and $Star^{-/-}$ mice was calculated using the ddCt method and examined using Student's t test, with a p value $<$0.05 considered significant. The transcriptome

TABLE 11.5 Genes Differentially Expressed in Knockout Mice Lacking StAR Compared with those in Wild-Type Mice by Quantitative Real-Time PCR

Functional Category	Gene	Description	FC (Mean ± SE)
Steroid hormone biosynthesis	*Nr5a1*	Nuclear receptor subfamily 5, group A, member 1	0.68 ± 0.52
	Mc2r	Melanocortin 2 receptor	0.29 ± 0.18
	Mrap	Melanocortin 2 receptor accessory protein	0.26 ± 0.51
	Star	Steroidogenic acute regulatory protein	0.02 ± 0.01*
	Cyp11a1	Cytochrome P450, family 11, subfamily a, polypeptide 1	0.63 ± 0.48
	Fdx1	Ferredoxin 1	0.63 ± 0.69
	Fdxr	Ferredoxin reductase	0.69 ± 0.56
	Hsd3b1	Hydroxy-delta-5-steroid dehydrogenase, 3 beta- and steroid delta-isomerase 1	0.51 ± 0.53
	Agtr1a	Angiotensin II receptor, type 1a	0.76 ± 0.58
	Ldlr	Low-density lipoprotein receptor	1.58 ± 1.19
	Scarb1	Scavenger receptor class B, member 1	1.39 ± 2.91
	Hmgcr	3-Hydroxy-3-methylglutaryl-Coenzyme A reductase	0.77 ± 0.31
	Lipe	Lipase, hormone sensitive	0.93 ± 0.45
Cholesterol biosynthesis and influx	*Npc2*	Niemann Pick type C2	3.46 ± 4.7
	Stard3	START domain containing 3	4.69 ± 3.15*
	Bzrpl1	Benzodiazapine receptor, peripheral-like 1	0.82 ± 0.94
	Srebf1	Sterol regulatory element binding factor 1	1.9 ± 0.93
	Acat2	Acetyl-Coenzyme A acetyltransferase 2	1.19 ± 1.08
	Nr1h2	Nuclear receptor subfamily 1, group H, member 2	3.04 ± 1.21*
	Nr1h3	Nuclear receptor subfamily 1, group H, member 3	7.76 ± 1.38*
	Abca1	ATP-binding cassette, sub-family A (ABC1), member 1	2.92 ± 1.59*
Cholesterol metabolism and efflux	*Abcg1*	ATP-binding cassette, sub-family G (WHITE), member 1	5.69 ± 3.1*
	Abcb1a	ATP-binding cassette, sub-family B (MDR/TAP), member 1A	0.37 ± 0.93
	Dhcr24	24-Dehydrocholesterol reductase	0.54 ± 0.62
	ch25h	Cholesterol 25-hydroxylase	0.57 ± 1.69
	Wt1	Wilms tumor homolog	1.83 ± 1.26
	Nr0b1	Nuclear receptor subfamily 0, group B, member 1	0.09 ± 0.10*
Adrenocortical development	*Shh*	Sonic hedgehog	0.02 ± 0.02*
	Wnt4	Wingless-related MMTV integration site 4	0.08 ± 0.06*

(Continued)

TABLE 11.5 (Continued)

Functional Category	Gene	Description	FC (Mean ± SE)
	Cd86	CD86 antigen	6.44 ± 3.39*
	Cd36	CD36 antigen	3.29 ± 2.03*
	Cd5l	CD5 antigen-like	130.95 ± 273.32*
	Spp1	Secreted phosphoprotein 1	259.15 ± 133.85*
	Ccl5	Chemokine (C-C motif) ligand 5	113.14 ± 144.27*
	Cxcl9	Chemokine (C-X-C motif) ligand 9	0.28 ± 1.23
	Clec7a	C-type lectin domain family 7, member a	100.69 ± 65.1*
Inflammatory response	*H2-Aa*	Histocompatibility 2, class II antigen A, alpha	36.41 ± 147.76
	H2-Ab1	Histocompatibility 2, class II antigen A, beta 1	24.29 ± 70.12
	H2-Ea	Histocompatibility 2, class II antigen E alpha	37.09 ± 475.29
	Tlr1	Toll-like receptor 1	4.12 ± 3.97
	Tlr2	Toll-like receptor 2	2.82 ± 2.31
	Tlr4	Toll-like receptor 4	2.08 ± 1.24
	Tlr6	Toll-like receptor 6	8.2 ± 8.33
	Tlr7	Toll-like receptor 7	4.59 ± 3.41

Asterisks (*) indicate statistically significant change ($p < 0.05$).
Modified data published by Ishii T, Mitsui T, Suzuki S, et al. Endocrinology *2012; 153: 2714–23.*

analysis and subsequent qPCR validation did not show significant differences between $Star^{+/+}$ and $Star^{-/-}$ mice in the expression of genes related to steroid hormone biosynthesis, other than *Star*, or cholesterol biosynthesis and influx. However, significant upregulation of the genes involved in cholesterol efflux, such as those encoding liver X receptors (LXRs) and adenosine triphosphate (ATP)-binding cassettes, was observed; significant downregulation of genes involved in adrenocortical development, such as dosage-sensitive sex reversal-adrenal hypoplasia critical region on X chromosome 1 (*Dax-1*; officially *Nr0b1*), wingless-related MMTV integration site 4 (*Wnt4*) and sonic hedgehog (*Shh*), was also observed (Table 11.5). These data reflect the pathophysiological features of adrenocortical cells upon StAR deficiency.

Pathway Analysis

Ishii *et al.* performed pathway analysis through IPA and NextBio.[34] IPA returned a list of canonical pathways most relevant to the transcriptome data set by a right- or two-tailed Fisher's exact probability test.[16] IPA identified significant associations between the DEGs and the canonical pathway of inflammatory or immune response, including dendritic cell maturation, antigen presentation pathway, allograft rejection

TABLE 11.6 Canonical Pathways Significantly Altered in Knockout Mice Lacking StAR Compared with those in Wild-Type Mice by Ingenuity Pathway Analysis

Canonical Pathway	*p*	Ratio
Dendritic cell maturation	2.13796E-10	2.27E-01
Antigen presentation pathway	1.41254E-09	3.72E-01
Allograft rejection signaling	1.62181E-08	2.00E-01
Role of NFAT in regulation of the immune response	1.90546E-08	2.21E-01
Altered T cell and B cell signaling in rheumatoid arthritis	2.51189E-08	2.86E-01
Graft-versus-host disease signaling	7.07946E-08	3.54E-01
PKCθ signaling in T lymphocytes	8.91251E-08	2.41E-01
Communication between innate and adaptive immune cells	0.0000001	2.23E-01
Systemic lupus erythematosus signaling	2.0893E-07	1.79E-01
CD28 signaling in T helper cells	2.51189E-07	2.48E-01
OX40 signaling pathway	6.76083E-07	2.04E-01
Autoimmune thyroid disease signaling	7.94328E-07	2.54E-01
TREM1 signaling	8.31764E-07	3.16E-01
Natural killer cell signaling	9.12011E-07	2.55E-01
B cell receptor signaling	1.62181E-06	2.33E-01
IL-4 signaling	1.99526E-06	3.00E-01
FcγRIIB signaling in b lymphocytes	2.51189E-06	3.02E-01
iCOS-iCOSL signaling in T helper cells	3.46737E-06	2.35E-01
Atherosclerosis signaling	4.36516E-06	2.40E-01
Glycosaminoglycan degradation	5.7544E-06	4.44E-01
Cytotoxic T lymphocyte-mediated apoptosis of target cells	1.02329E-05	1.88E-01
B cell development	1.54882E-05	2.97E-01
Fcγ receptor-mediated phagocytosis in macrophages and monocytes	1.77828E-05	2.53E-01
T helper cell differentiation	2.39883E-05	2.68E-01
Role of pattern recognition receptors in recognition of bacteria and viruses	3.16228E-05	2.56E-01
PI3K signaling in B lymphocytes	3.46737E-05	2.13E-01
Crosstalk between dendritic cells and natural killer cells	5.49541E-05	2.17E-01
Type I diabetes mellitus signaling	5.7544E-05	2.14E-01
LXR/RXR activation	6.76083E-05	2.41E-01
Leukocyte extravasation signaling	7.24436E-05	1.91E-01

(Continued)

TABLE 11.6 (Continued)

Canonical Pathway	*p*	Ratio
IL-8 signaling	8.31764E-05	1.94E-01
Production of nitric oxide and reactive oxygen species in macrophages	0.000147911	1.98E-01
IL-10 signaling	0.000165959	2.50E-01
Role of BRCA1 in DNA damage response	0.000165959	2.71E-01
CTLA4 signaling in cytotoxic T lymphocytes	0.000190546	2.16E-01
IL-12 signaling and production in macrophages	0.000190546	1.98E-01
T cell receptor signaling	0.000436516	2.14E-01
fMLP signaling in neutrophils	0.000489779	1.95E-01
Sphingolipid metabolism	0.000537032	2.14E-01
NF-κB activation by viruses	0.000630957	2.28E-01
Renin-angiotensin signaling	0.000977237	2.02E-01
NF-κB signaling	0.00128825	1.71E-01
Role of JAK1 and JAK3 in γc cytokine signaling	0.001513561	2.27E-01
MSP-RON signaling pathway	0.001584893	2.50E-01
Phospholipase C signaling	0.001659587	1.53E-01
Primary immunodeficiency signaling	0.001778279	1.75E-01
Erythropoietin signaling	0.001778279	2.16E-01
Virus entry via endocytic pathways	0.001862087	2.04E-01
Role of macrophages, fibroblasts and endothelial cells in rheumatoid arthritis	0.002511886	1.41E-01
Phospholipid degradation	0.002754229	2.10E-01

p values are calculated by Fischer's exact probability test.
Ratios indicate the number of differentially expressed genes by total number of genes that map to the pathway.

signaling, communication between innate and adaptive immune cells, and interleukin (IL)-4 signaling (Table 11.6). NextBio identified a list of biogroups or cell types most significantly correlated with the transcriptome data set by Fisher's exact probability test with a multiple comparison test.[15] The NextBio analysis identified immune response as the most significant biogroup. The NextBio analysis identified macrophages from the peripheral tissues of C57BL/6 mice, microglial cells from C57BL/6 mice, and follicular dendritic cells from the lymph nodes of BALB/cAnNCrlCrlj mice as the most significant cell types positively correlated with the DEGs (Table 11.7). Both pathway analyses consistently indicated that the inflammatory or immune response was significantly altered in the adrenocortical cells of $Star^{-/-}$ mice.

TABLE 11.7 Cell types Significantly Altered in Knockout Mice Lacking StAR Compared with those in Wild-Type Mice by NextBio

Cell Type	Body System	Score	Correlation	*p*
Macrophage of peripheral tissue of C57BL/6 strain	Immune	263.88	+	2.50E-115
Microglial cell of C57BL/6 strain	Immune	255.83	+	7.8E-112
Dendritic cell follicular of lymph node of BALB/cAnNCrlCrlj strain	Immune	238.97	+	1.60E-104
Macrophage of bone marrow of C57BL/6 strain	Immune	217.19	+	4.7E-95
Dendritic cell (CD11c+ CD11b_hi CD103-) of lung of BALB/cByJ strain	Immune	214.96	+	4.40E-94
Myeloid-derived suppressor cell (CD11b+) of spleen of BALB/c strain	Immune	208.02	+	4.6E-91
Macrophage of peritoneum of C57BL/6J strain	Immune	187.31	+	4.50E-82
Osteoclast of C57BL/6 strain	Musculoskeletal	180.83	+	2.9E-79
Dendritic cell of bone marrow of 129SvJae x C57BL/6 strain	Immune	173.11	+	6.60E-76
Macrophage of peritoneum of C57BL/6 strain	Immune	170.00	+	1.5E-74
Dendritic cell of bone marrow of C57BL/6 strain	Immune	160.33	+	2.30E-70
Monocyte (Ly6c_hi) of peripheral blood of C57BL/6 strain	Immune	156.61	+	9.60E-69
Macrophage (CD11c_int CD11b + B220- CD4- CD8- CD169_hi F4/80+) of lymph node medulla of C57BL/6 strain	Immune	154.21	+	1.1E-67
Monocyte (Ly6c_lo) of peripheral blood of C57BL/6 strain	Immune	150.70	+	3.60E-66
Hematopoietic stem cell (CD45+ Sca1+) of muscle of C57BL/6 strain	Immune	146.86	+	1.7E-64
Macrophage (CD11b+ CD11c-) of lamina propria of small intestine of C57BL/6 strain	Immune	146.40	+	2.60E-64
Dendritic cell (CD11c+) of bone marrow of C57BL/6J strain	Immune	140.43	+	1E-61
Dendritic cell (myeloid CD8a-) of C57BL/6 strain	Immune	133.03	+	1.70E-58
Macrophage of mammary gland of FVB/N strain	Exocrine	130.98	+	1.3E-57

(Continued)

TABLE 11.7 (Continued)

Cell Type	Body System	Score	Correlation	p
Dendritic cell of bone marrow of BALB/c strain	Immune	127.28	+	5.30E-56
Macrophage (CD11b+ CD11c-) cell of spleen of C57BL/6 strain	Immune	126.92	+	7.6E-56
Neutrophil (lineage- c-kit- Gr1+ Mac1+) of bone marrow of C57BL/6 strain	Immune	125.64	+	2.70E-55
Monocyte (Mac1 +) of peripheral blood of C57BL/6 strain	Immune	123.10	+	3.5E-54
Dendritic cell of lymph node of BALB/c strain	Immune	120.18	+	6.40E-53
Dendritic cell (CD11c_hi CD11b+ CD19- CD3- NK1.1- 120G8_lo) of spleen of C57BL/6 strain	Immune	114.76	+	1.5E-50
Dendritic cell (CD11c + CD11b_lo CD103 +) of lung of BALB/cByJ strain	Immune	112.02	+	2.30E-49
Dendritic cell (CD8- 33D1 + CD205- CD11c +) of spleen of C57BL/6 strain	Immune	110.27	+	1.3E-48
Dendritic cell of spleen of BALB/c strain	Immune	110.03	+	1.60E-48
Spermatagonial cell (Thy1-) of testis of C57BL/6 strain	Urogenital	108.87	−	5.2E-48
Dendritic cell (plasmacytoid CD11c_int CD19- CD3- NK1.1- 120G8_hi) of spleen of C57BL/6 strain	Immune	105.74	+	1.20E-46
B lymphocyte (B220 +) of spleen of C57BL/6 strain	Immune	103.87	+	7.7E-46
Synovial fibroblast of knee joint of BALB/c strain	Musculoskeletal	103.11	+	1.70E-45
Dendritic cell (CD8 + 33D1- CD205 + CD11c +) of spleen of C57BL/6 strain	Immune	101.76	+	6.4E-45
Macrophage of bone marrow of BALB/c strain	Immune	101.51	+	8.20E-45
Myeloid-derived suppressor cell (CD11b +) of bone marrow of BALB/c strain	Immune	100.95	+	1.4E-44
Stem cell of spermatagonia of C57BL/6J strain	Urogenital	98.10	−	2.50E-43
Side population cell of tibialis anterior muscle of C57BL/6 strain	Musculoskeletal	93.86	+	1.7E-41
Cardiac progenitor cell of ROSA26 x Isl1 strain	Cardiovascular	91.09	−	2.80E-40

(*Continued*)

TABLE 11.7 (Continued)

Cell Type	Body System	Score	Correlation	*p*
Type II cell of lung of ICR10 strain	Respiratory	87.77	+	7.7E-39
Dendritic cell (IFN-producing killer) of lymph node of BALB/c strain	Immune	87.54	+	9.60E-39
Dendritic cell (CD11c+) of lamina propria of C57BL/6 strain	Immune	87.03	+	1.6E-38
B lymphocyte (B220+ CD19+ IgM+) of spleen of C57BL/6 strain	Immune	85.93	+	4.80E-38
Dendritic cell of Peyer's patch of BALB/c strain	Immune	84.02	+	3.2E-37
Mesenchymal cell of proximal forelimb of of CD-1 strain	Integumentary	83.27	−	6.90E-37
Granulocyte (lineage- Gr-1+ clone7.4+) of bone marrow of C57BL/6 strain	Immune	82.65	+	1.3E-36
T lymphocyte (CD4+) of undetermined strain	Immune	82.12	+	2.20E-36
Dendritic cell (CD8 −) of spleen of C57BL/6 strain	Immune	81.97	+	2.5E-36
Granulosa cell of ovary of C57BL/6J x 129S5/SvEvBrd strain	Urogenital	81.23	−	5.30E-36
Mesenchymal cell of distal hindlimb of CD-1 strain	Integumentary	81.03	−	6.4E-36
Mesothelial cell (Mesothelin +) of liver of C57BL/6 strain	Digestive	80.84	+	7.80E-36

The correlation score represents the magnitude of correlation between gene expression profiles, computed with the Running Fisher algorithm, a non-parametric rank-based statistical approach.
Symbols of + and − indicate positive and negative correlation, respectively.
p values are calculated by Fischer's exact probability test.

Pathophysiological Hallmarks Identified by the Transcriptome Analysis of the Adrenocortical Cells of *Star*$^{-/-}$ Mice

In the study by Ishii *et al.*, genes involved in the inflammatory or immune response, the LXR signaling, and the adrenocortical zonation show a significant positive correlation with the DEGs in *Star*$^{-/-}$ mice-derived adrenocortical cells.[34] The results provide useful information to elucidate the pathophysiology of adrenocortical cells in patients with lipoid CAH.

Inflammatory or Immune Response

The inflammatory or immune response may play a physiological role in adrenocortical cells, especially under stress conditions. Woods and Judd reported that IL-4 signaling inhibited the expression of ACTH-induced steroidogenic

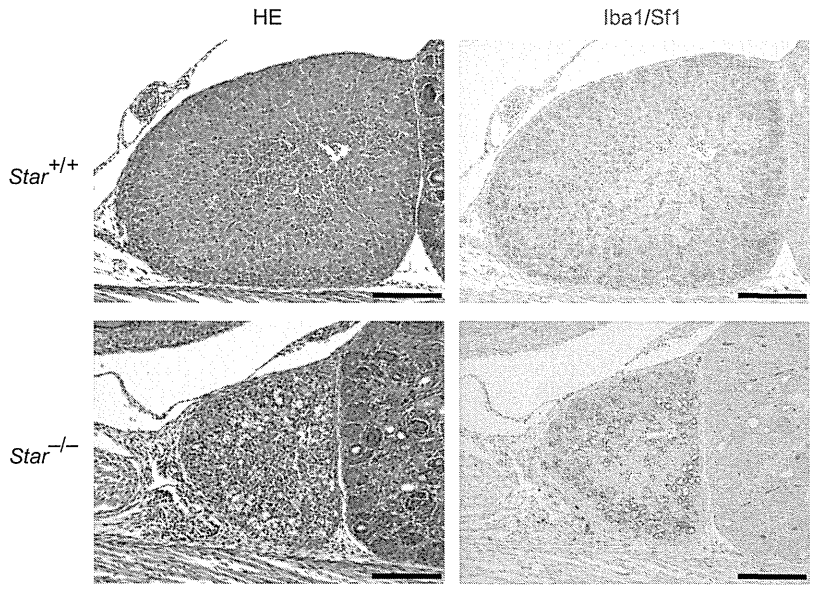

FIGURE 11.3 Immunohistochemistry for Iba1 (a macrophage marker) and *in situ* hybridization for Nr5a1 (a steroidogenic cell marker) in the adrenal glands at E18.5. Red and blue staining represents Iba1 immunoreactivity and Nr5a1 transcripts, respectively. Scale bars are 200 μm. HE, hematoxylin and eosin staining.

enzymes in bovine zona reticularis cells.[36] IL-4 signaling is one of the canonical pathways in which genes are significantly upregulated in $Star^{-/-}$ mice (Table 11.6). The increased inflammatory or immune response, including IL-4 signaling, could be the second "hit" of the two-hit model for lipoid CAH, attenuating the signal transduction of melanocortin type 2 receptor under high levels of circulating ACTH. The actual role of the inflammatory or immune response in the adrenocortical cells of $Star^{-/-}$ mice remains unclear.

Based on the results of transcriptome analysis, the expression pattern of a specific macrophage marker, Iba1, was examined in the adrenal glands by immunohistochemical analysis.[37] Fixed whole embryos at E17.5–18.5 were double-stained by immunohistochemistry and *in situ* hybridization for markers of macrophages (Iba1; officially Aif1, allograft inflammatory factor 1) and steroidogenic cells (*Sf1*; officially *Nr5a1*), respectively. Iba1 immunoreactivity was detected in only several *Sf1*-negative resident macrophages within the adrenal cortex of $Star^{+/+}$ mice, but in a larger number of *Sf1*-negative resident macrophages within the adrenal cortex of $Star^{-/-}$ mice (Figure 11.3).

These findings suggest a link between the inflammatory or immune system and the adrenal glands. Adrenocortical cells produce various cytokines during acute stress.[38] Additionally, intra-adrenal macrophages influence the function of the adrenal gland in an autocrine or paracrine manner.[38] As shown in Figure 11.3, many macrophages infiltrated into the adrenal glands of $Star^{-/-}$ mice.[34] $Star^{-/-}$ mice-derived adrenocortical cells exhibited significantly higher mRNA levels of chemokine ligand 5 (Ccl5) and CD36 antigen (Cd36) than cells from $Star^{+/+}$ mice.[34] Ccl5, an adipocytokine, recruits macrophages into adipose tissues.[39] CD36, a receptor for apoptosis inhibitor of macrophage (AIM), induces lipolysis and chemokine production in adipocytes.[40] These data suggest a reciprocal

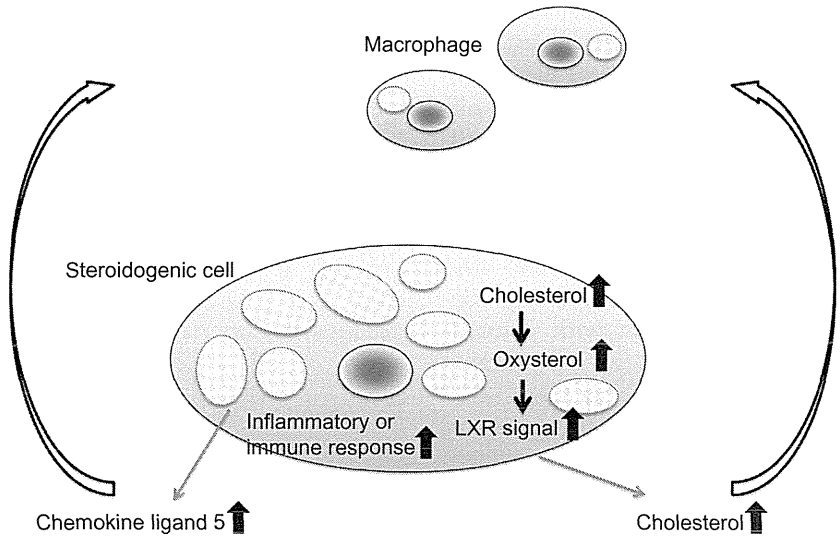

FIGURE 11.4 **Schematic model of "adrenal remodeling" in *Star*$^{-/-}$ mice.** Upward arrow indicates an increased number of molecules or transcripts involved in the index pathways. Blue ovals indicate nuclei; yellow ovals indicate lipid droplets of cholesterol ester in the cytoplasm of adrenocortical cells or macrophages. LXR, liver X receptor.

interaction between adrenocortical cells and infiltrated macrophages upon disruption of StAR. The adrenal glands of *Star*$^{-/-}$ mice may share some features of homeotic inflammation with white adipose tissue in patients with obesity and with vascular walls in those with atherosclerosis,[41–43] which can be called "adrenal remodeling" (Figure 11.4).

LXR Signaling

Significant upregulation of LXRs α and β (Nr1h3 and Nr1h2, respectively) has been observed in *Star*$^{-/-}$ mice-derived adrenocortical cells whose cytoplasms are filled with cholesterol esters.[34] Cummins *et al.* reported that knockout mice lacking LXRs α and β (*Lxrαβ*$^{-/-}$ mice) accumulated cholesterol esters.[44] Hence, it has been inferred that LXRs α and β play an important role in protecting adrenal glands from the accumulation of free cholesterol. Accumulated oxysterol intermediates could function as ligands for LXRs in the adrenocortical cells of *Star*$^{-/-}$ mice and induce cholesterol efflux by increasing the expression of ATP-binding cassettes (Abca1 and Abcg1). Furthermore, enhanced LXR signaling could inhibit the expression of multiple steroidogenic genes, as reported in the H295R human adrenocortical cell line.[45] Cummins *et al.* showed increased adrenal steroidogenesis even with a decline of StAR expression in *Lxrαβ*$^{-/-}$ mice,[44] indicating a possible link between the repression of LXR signaling and the increase in StAR-independent steroidogenesis. These findings give additional credence to the role of LXRs in maintaining cholesterol homeostasis in adrenocortical cells and imply that LXR upregulation is relevant to the lost residual capacity for StAR-independent steroidogenesis as the second hit in the two-hit model for lipoid CAH.

Adrenocortical Zonation

Genes related to the transition from fetal to adult adrenocortical cells are significantly downregulated in *Star*$^{-/-}$ mice-derived adrenocortical cells.[34] The adult cortex ultimately develops from precursor cells in the fetal cortex, as shown

by a lineage tracing study by Morohashi's laboratory.[46] The adult cortex is then maintained through proliferation and the clonal replenishment of subcapsular progenitor or stem cells that probably move centripetally and differentiate into steroidogenic cells in the zona glomerulosa or fasciculata.[22,47–49] Consistent with these ideas, the adrenal glands of *Star*$^{-/-}$ mice are severely hypoplastic during embryonic and early neonatal stages, and are definitely disturbed during cortical zonation with disorganized mitochondria,[31] similar to the adrenal glands of knockout mice lacking Cyp11a1.[50] Although StAR expression in adrenocortical progenitor or stem cells remains undetermined, decreased expression of the genes related to adrenocortical cell development in steroidogenic cells could directly or indirectly disturb normal proliferation and differentiation in the adrenal cortex of *Star*$^{-/-}$ mice.

PERSPECTIVE

Transcriptome analysis allows for simultaneous investigation of an entire set of transcripts and permits parallel comparisons between different cells, such as healthy and diseased cells. As shown in this chapter, transcriptome analysis has helped identify significant alteration of gene expression associated with the inflammatory or immune response, the cholesterol efflux, and the adrenocortical zonation in the adrenocortical cells of *Star*$^{-/-}$ mice. However, mRNA level may not always correlate with the biological function or phenotype of the cells. Biological function or phenotype is also affected by the corresponding protein level and modification. Bearing these limitations in mind, transcriptome analysis is a useful strategy for identifying hitherto undescribed functions or pathways to identify new pathophysiology or therapeutic approaches. If appropriately applied, global profiling of transcripts will provide an essential tool for future research on the nature of adrenocortical cells.

Acknowledgements

This work was supported by a Grant-in-Aid for Scientific Research (C) from the Japan Society for the Promotion of Science, a Health Science Research Grant for Research on Applying Health Technology (Jitsuyoka (Nanbyo)-Ippan-014) from the Ministry of Health, Labor and Welfare, Japan, and a Research Grant from the Yamaguchi Endocrine Research Foundation.

References

1. Venter JC, Adams MD, Myers EW, et al. The sequence of the human genome. *Science* 2001;**291**:1304–51.
2. Lander ES, Linton LM, Birren B, et al. Initial sequencing and analysis of the human genome. *Nature* 2001;**409**:860–921.
3. Mouse Genome Sequencing Consortium, Waterston RH, Lindblad-Toh K, et al. Initial sequencing and comparative analysis of the mouse genome. *Nature* 2002;**420**:520–62.
4. Zhang W, Morris QD, Chang R, et al. The functional landscape of mouse gene expression. *J Biol* 2004;**3**:21.
5. Shalon D, Smith SJ, Brown PO. A DNA microarray system for analyzing complex DNA samples using two-color fluorescent probe hybridization. *Genome Res* 1996;**6**:639–45.
6. MAQC Consortium, Shi L, Reid LH, et al. The MicroArray Quality Control (MAQC) project shows inter- and intraplatform reproducibility of gene expression measurements. *Nat Biotechnol* 2006;**24**:1151–61.
7. Shi L, Campbell G, Jones WD, et al. The MicroArray Quality Control (MAQC)-II study of common practices for the development and validation of microarray-based predictive models. *Nat Biotechnol* 2010;**28**:827–38.
8. Wang Z, Gerstein M, Snyder M. RNA-Seq: a revolutionary tool for transcriptomics. *Nat Rev Genet* 2009;**10**:57–63.
9. Costa V, Aprile M, Esposito R, Ciccodicola A. RNA-Seq and human complex diseases: recent accomplishments and future perspectives. *Eur J Hum Genet* 2013;**21**:134–42.
10. Grewal A, Lambert P, Stockton J. Analysis of expression data: an overview. In: Baxevanis AD, editor. *Current protocols in bioinformatics*. New York: John Wiley; 2007.
11. Benjamini Y, Hochberg Y. Controlling the false discovery rate: a practical and powerful approach to multiple testing. *J R Stat Soc Series B Stat Methodol* 1995;**45**:486–90.

12. Reiner A, Yekutieli D, Benjamini Y. Identifying differentially expressed genes using false discovery rate controlling procedures. *Bioinformatics* 2003;**19**: 368–75.
13. Gene Ontology Consortium. The Gene Ontology project in 2008. *Nucleic Acids Res* 2008;**36**:D440–4.
14. Kanehisa M, Goto S, Kawashima S, Okuno Y, Hattori M. The KEGG resource for deciphering the genome. *Nucleic Acids Res* 2004;**32**:D277–80.
15. Kupershmidt I, Su QJ, Grewal A, et al. Ontology-based meta-analysis of global collections of high-throughput public data. *PLoS One* 2010;**5**:e13066.
16. Salomonis N, Hanspers K, Zambon AC, et al. GenMAPP 2: new features and resources for pathway analysis. *BMC Bioinformatics* 2007;**8**:217.
17. Miller WL, Auchus RJ. The molecular biology, biochemistry, and physiology of human steroidogenesis and Its disorders. *Endocr Rev* 2011;**32**:81–151.
18. Lee JJ, Widmaier EP. Gene array analysis of the effects of chronic adrenocorticotropic hormone in vivo on immature rat adrenal glands. *J Steroid Biochem Mol Biol* 2005;**96**:31–44.
19. Meyer JS. Biochemical effects of corticosteroids on neural tissues. *Physiol Rev* 1985;**65**:946–1020.
20. Schimmer BP, Cordova M, Cheng H, et al. Global profiles of gene expression induced by adrenocorticotropin in Y1 mouse adrenal cells. *Endocrinology* 2006;**147**:2357–67.
21. Lotfi CFP, Todorovic Z, Armelin HA, Schimmer BP. Unmasking a growth-promoting effect of the adrenocorticotropic hormone in Y1 mouse adrenocortical tumor cells. *J Biol Chem* 1997;**272**:29886–91.
22. Kim AC, Barlaskar FM, Heaton JH, et al. In search of adrenocortical stem and progenitor cells. *Endocr Rev* 2009;**30**:241–63.
23. Nishimoto K, Rigsby CS, Wang T, et al. Transcriptome analysis reveals differentially expressed transcripts in rat adrenal zona glomerulosa and zona fasciculata. *Endocrinology* 2012;**153**:1755–63.
24. Heikkilä M, Peltoketo H, Leppäluoto J, Ilves M, Vuolteenaho O, Vainio S. Wnt-4 deficiency alters mouse adrenal cortex function, reducing aldosterone production. *Endocrinology* 2002;**143**:4358–65.
25. Mandel H, Shemer R, Borochowitz ZU, et al. SERKAL syndrome: an autosomal-recessive disorder caused by a loss-of-function mutation in WNT4. *Am J Hum Genet* 2008;**82**:39–47.
26. Artemenko IP, Zhao D, Hales DB, Hales KH, Jefcoate CR. Mitochondrial processing of newly synthesized steroidogenic acute regulatory protein (StAR), but not total StAR, mediates cholesterol transfer to cytochrome P450 side chain cleavage enzyme in adrenal cells. *J Biol Chem* 2001;**276**:46583–96.
27. Jefcoate C. High-flux mitochondrial cholesterol trafficking, a specialized function of the adrenal cortex. *J Clin Invest* 2002;**110**:881–90.
28. Clark BJ, Wells J, King SR, Stocco DM. The purification, cloning, and expression of a novel luteinizing hormone-induced mitochondrial protein in MA-10 mouse Leydig tumor cells. Characterization of the steroidogenic acute regulatory protein (StAR). *J Biol Chem* 1994;**269**:28314–22.
29. Bose HS, Sugawara T, Strauss JF, Miller WL. The pathophysiology and genetics of congenital lipoid adrenal hyperplasia. *N Engl J Med* 1996;**335**:1870–8.
30. Hasegawa T, Zhao L, Caron KM, et al. Developmental roles of the steroidogenic acute regulatory protein (StAR) as revealed by StAR knockout mice. *Mol Endocrinol* 2000;**14**:1462–71.
31. Ishii T, Hasegawa T, Pai C-I, et al. The roles of circulating high-density lipoproteins and trophic hormones in the phenotype of knockout mice lacking the steroidogenic acute regulatory protein. *Mol Endocrinol* 2002;**16**:2297–309.
32. Sasaki G, Ishii T, Jeyasuria P, et al. Complex role of the mitochondrial targeting signal in the function of steroidogenic acute regulatory protein revealed by bacterial artificial chromosome transgenesis *in vivo*. *Mol Endocrinol* 2008;**22**:951–64.
33. Caron KM, Soo SC, Wetsel WC, Stocco DM, Clark BJ, Parker KL. Targeted disruption of the mouse gene encoding steroidogenic acute regulatory protein provides insights into congenital lipoid adrenal hyperplasia. *Proc Natl Acad Sci USA* 1997;**94**:11540–5.
34. Ishii T, Mitsui T, Suzuki S, Matsuzaki Y, Hasegawa T. A genome-wide expression profile of adrenocortical cells in knockout mice lacking steroidogenic acute regulatory protein. *Endocrinology* 2012;**153**:2714–23.
35. ten Hagen TL, van Vianen W, Bakker-Woudenberg IA. Isolation and characterization of murine Kupffer cells and splenic macrophages. *J Immunol Methods* 1996;**193**:81–91.
36. Woods AM, Judd AM. Interleukin-4 increases cortisol release and decreases adrenal androgen release from bovine adrenal cells. *Domest Anim Endocrinol* 2008;**34**:372–82.
37. Kanazawa H. Macrophage/microglia-specific protein Iba1 enhances membrane ruffling and Rac activation via phospholipase C-γ-dependent pathway. *J Biol Chem* 2002;**277**:6–32.
38. Bornstein SR, Rutkowski H, Vrezas I. Cytokines and steroidogenesis. *Mol Cell Endocrinol* 2004;**215**:135–41.
39. Keophiphath M, Rouault C, Divoux A, Clement K, Lacasa D. CCL5 promotes macrophage recruitment and survival in human adipose tissue. *Arterioscler Thromb Vasc Biol* 2009;**30**:39–45.

40. Kurokawa J, Nagano H, Ohara O, et al. Apoptosis inhibitor of macrophage (AIM) is required for obesity-associated recruitment of inflammatory macrophages into adipose tissue. *Proc Natl Acad Sci USA* 2011;**108**:12072–7.
41. Gregor MF, Hotamisligil GS. Inflammatory mechanisms in obesity. *Annu Rev Immunol* 2011;**29**:415–45.
42. Rocha VZ, Libby P. Obesity, inflammation, and atherosclerosis. *Nat Rev Cardiol* 2009;**6**:399–409.
43. Suganami T, Ogawa Y. Adipose tissue macrophages: their role in adipose tissue remodeling. *J Leukoc Biol* 2010;**88**:33–9.
44. Cummins C, Mangelsdorf D. Liver X receptors and cholesterol homoeostasis: spotlight on the adrenal gland. *Biochem Soc Trans* 2006;**34**:1110–3.
45. Nilsson M, Stulnig TM, Lin C-Y, et al. Liver X receptors regulate adrenal steroidogenesis and hypothalamic-pituitary-adrenal feedback. *Mol Endocrinol* 2007;**21**: 126–37.
46. Zubair M, Parker KL, Morohashi K-I. Developmental links between the fetal and adult zones of the adrenal cortex revealed by lineage tracing. *Mol Cell Biol* 2008;**28**:7030–40.
47. King P, Paul A, Laufer E. Shh signaling regulates adrenocortical development and identifies progenitors of steroidogenic lineages. *Proc Natl Acad Sci USA* 2009;**106**:21185–90.
48. Huang C-CJ, Miyagawa S, Matsumaru D, Parker KL, Yao HH-C. Progenitor cell expansion and organ size of mouse adrenal is regulated by sonic hedgehog. *Endocrinology* 2010;**151**:1119–28.
49. Ching S, Vilain E. Targeted disruption of Sonic Hedgehog in the mouse adrenal leads to adrenocortical hypoplasia. *Genesis* 2009;**47**:628–37.
50. Hu M-C, Hsu N-C, El Hadj NB, et al. Steroid deficiency syndromes in mice with targeted disruption of Cyp11a1. *Mol Endocrinol* 2002;**16**:1943–50.

2 成長ホルモンと身長増加

成長ホルモンとは

成長ホルモン（growth hormone：GH）は，hGH-N 遺伝子にコードされるペプチドホルモンである（❶）．hGH-N 遺伝子は下垂体前葉の somatotroph 細胞でのみ発現するので，GH の合成場所は下垂体前葉に限られる．下垂体の細胞の約 40％が somatotroph 細胞である．GH は 191 個のアミノ酸残基から成る 22 kDa の一本鎖ポリペプチドであるが，血中 GH の 10％程度は，alternative splicing により生じる，15 個のアミノ酸残基を欠く 20 kDa GH である．両者の成長促進効果は同等であるとされている．

❶ 染色体 17q22-24 に位置する GH 遺伝子クラスター

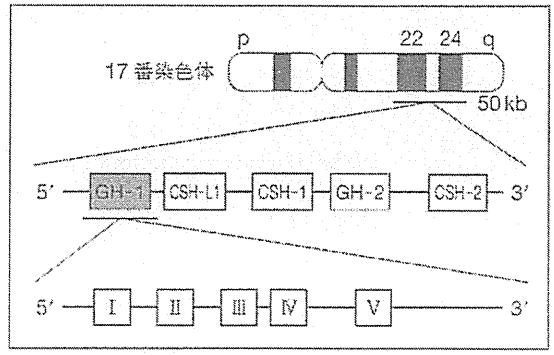

おのおのの遺伝子は 90％以上の相同性があり，5 つのエクソンと 4 つのイントロンをもつ．
GH-1（または GH-N）：下垂体のみで発現．
GH-2（または GH-V）：胎盤 syncytiotrophoblast で発現．
CSH-1, 2［chorionic somatomammotropin hormone-1, 2（または CSA, CSB）］：胎盤 trophoblast で発現．
CSH-L1［CSH-like-1］：偽遺伝子．

成長ホルモンの分泌

GH の合成と放出は，成長ホルモン放出ホルモン（growth hormone releasing hormone：GHRH）やソマトスタチン，グレリン（Ghrelin），インスリン様成長因子 I（insulin-like growth factor I：IGF-I），甲状腺ホルモン，グルココルチコイドなどの調節を受けている[1]（❷）．

視床下部性の主要な調節因子は GHRH とソマトスタチンである．GHRH を持続的に投与しても GH パルス（脈動的分泌）は維持されるので，ソマトスタチンがパルス生成に主要な役割を果たしていると考えられている．GHRH は，GH 遺伝子の転写と，GH の分泌を促進する．

グレリンは胃粘膜などの末梢組織，および一部は視床下部で合成されるペプチドで，視床下部からの GHRH 分泌と下垂体からの GH 分泌

Consideration points

成長ホルモンは，骨の伸長以外にも多くの生理的役割をもつ

❶ 成長ホルモンの骨伸長には，IGF-I を介する機序と，GH の直接作用の両方が関与する．
❷ 成長ホルモンは，筋肉においては筋量増加・糖新生促進に働き，脂肪組織では脂肪分解を促進するなど，骨伸長以外にも重要な生理的役割をもつ．
❸ したがって，成長が終了した成人期であっても，重度の成長ホルモン不足は治療の対象となる．

❷ 視床下部-下垂体での GH 分泌調節と，末梢組織での GH，IGF-I の作用

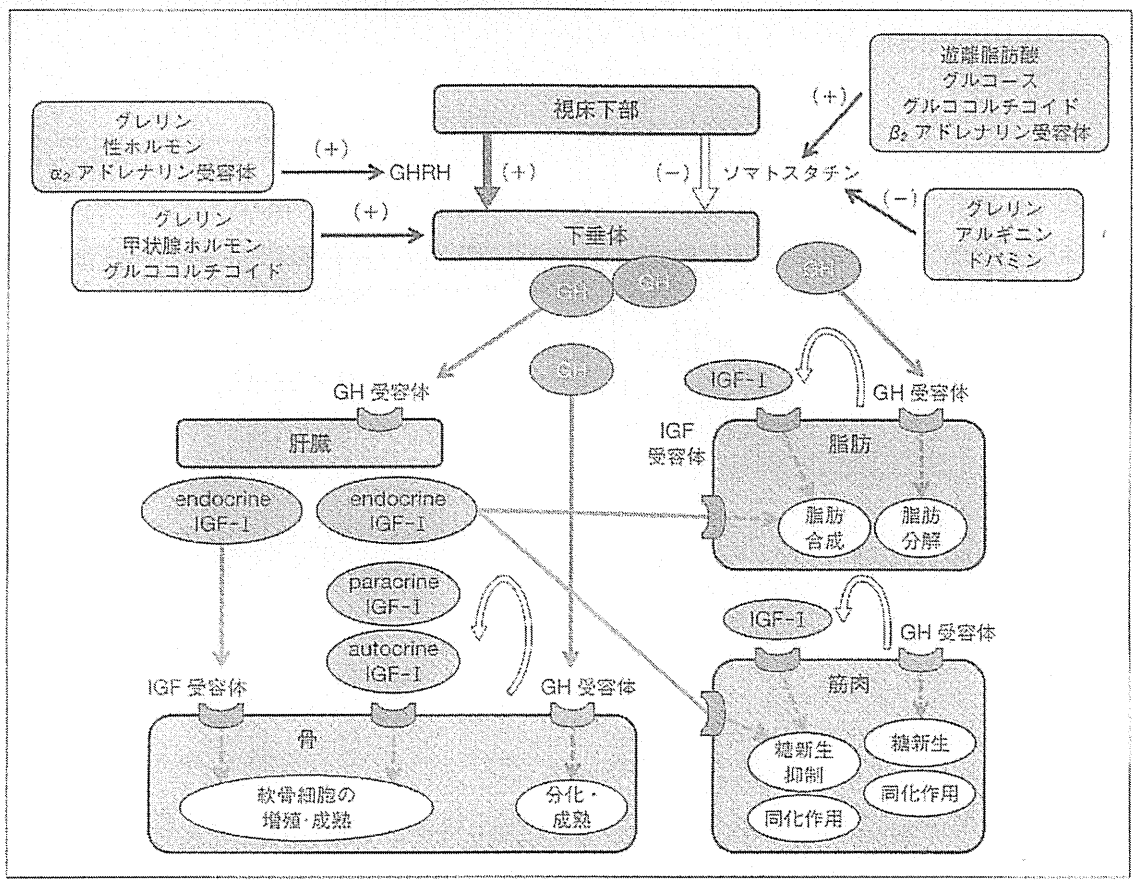

下垂体からの GH 分泌は，主として GHRH とソマトスタチンにより規定されており，グレリンや性ホルモンなど多くの因子により修飾される．
IGF-I は，肝臓で合成される endocrine IGF-I と，末梢由来の autocrine/paracrine IGF-I に区分される．GH と IGF-I は，骨・筋の同化作用において共同的に働く一方で，一部では拮抗的に作用する．

を刺激する．この作用は，GHS（GH secretagogue）受容体を介して発揮される．GHRH 受容体と GHS 受容体とは，別個の細胞内情報伝達経路を利用しているので，飽和量の GHRH 投与後でも，GHS により GH 分泌はさらに増加する．GHS 受容体を刺激する人工ペプチドがいくつか合成され（GHPR-2 など），GH 分泌不全症の診断に用いられている．

❷ 以外にも，情動，睡眠，食事，肥満，血糖変動などの多彩な因子が GH 分泌に関与している．

成長ホルモンと IGF-I

GH の生理作用は，成長および代謝の調節である．GH 受容体（GHR）は肝臓に豊富に存在するほか，筋肉や脂肪組織などの末梢組織にも認められる．GH 受容体は，cytokine/hematopoietin 受容体スーパーファミリーに属し，主として JAL/STAT カスケード（とくに STAT-1, 3, 5）のリン酸化により細胞内情報伝達を行っている．

GH の成長促進作用は，軟骨細胞に対する GH の直接作用と，IGF-I が介在するものに大別される（❷）．さらに IGF-I は，肝臓で合成されて血液中を循環する endocrine IGF-I と，末梢組織で産生され局所で作用する autocrine/paracrine IGF-I に区分される．IGF-I 遺伝子を肝臓特異的に欠失したマウスでは，血中 IGF-I 濃度は対照の 25％に低下するが，成長は正常

であったことから，成長促進作用には autocrine/paracrine IGF-I の関与が大きいと考えられている[2]．

❷に示すように，軟骨細胞増殖に対しては，GH と IGF-I は共同的に作用するが，骨外での代謝作用では一部逆に作用することもある[3]．たとえば脂肪組織では，GH が脂肪分解を促進するのに対し，IGF-I は脂肪合成に働く．筋組織でも，GH が糖新生促進に作用し，IGF-I は糖新生抑制方向に働いている．

GH 分泌不全を有する成人（adult GHD）では，除脂肪体重（lean body mass）の低下，体脂肪の増加，血中総コレステロールと LDL コレステロールの上昇，骨密度の低下などが認められる[1]．

血中での存在様式

GH

循環血中の 22 kDa GH の約 50％は，60 kDa high-affinity GHBP（GH 結合タンパク）と結合している．この GHBP は，GH 受容体の細胞外ドメインと同一である．20 kDa GH のほうは，20 kDa low-affinity GHBP と優先的に結合する．GHBP の生理的役割として，腎からの喪失の抑制による半減期の延長や，急激な血中濃度変動の防止などが想定されている．

IGF-I

血中では，IGF-I は IGF 結合タンパク-3（IGFBP-3）および acid-labile subunit（ALS）とともに三量体を形成している．このような形態をとることで，IGF-I 半減期の延長，IGF 受容

❹ 日本人小児における血清 IGF-I 濃度基準値（ng/mL）

年齢（歳）	男性					女性				
	−2 SD	−1 SD	中央値	+1 SD	+2 SD	−2 SD	−1 SD	中央値	+1 SD	+2 SD
0	11	35	67	105	149	15	38	69	107	154
1	14	38	69	106	148	23	49	85	130	186
2	18	42	74	111	154	32	60	99	150	213
3	24	50	82	120	164	40	69	108	161	227
4	32	60	93	132	176	48	77	116	169	238
5	44	73	108	148	193	56	86	126	181	252
6	55	86	124	166	215	69	102	147	207	287
7	63	99	142	192	247	89	129	183	257	357
8	72	114	165	225	292	111	159	224	314	438
9	84	134	195	267	350	133	188	264	370	517
10	99	159	233	321	423	155	217	302	422	588
11	113	184	272	377	499	175	241	333	460	638
12	125	203	301	419	557	188	255	348	476	654
13	133	214	315	436	579	193	259	349	473	643
14	138	217	315	433	570	193	257	344	463	625
15	141	217	310	422	552	192	256	341	456	614
16	142	216	307	416	543	192	255	340	455	611
17	142	216	306	414	540	191	252	335	447	599
18	142	214	301	405	526	188	247	326	431	574
19	143	210	292	389	501	182	238	311	408	539
20	142	204	280	368	470	175	226	293	381	499

（Isojima T, et al. 2012[5]）